Electronic Supplementary Material (ESI) for Journal of Materials Chemistry B.

Supporting Information

Developing a pH-sensitive $Al(OH)_3$ layer mediated UCNP@$Al(OH)_3$/Au nanohybrids for photothermal therapy and fluorescence imaging in vivo

Jian Chen [a, 1], Dongya Zhang [a, 1], Yan Zou [a], Zhongjie Wang [a], Mingcong Hao [a], Meng Zheng [a], Xue Xue [b], Xiaoxi Pan [c], Yiqing Lu [a], Jiefei Wang [a, *], Bingyang Shi [a, *]

[a] International Joint Center for Biomedical Innovation, Henan University, Kaifeng 475004, China.

[b] State Key Laboratory of Medicinal Chemical Biology and College of Pharmacy, Nankai University, Tianjin 300350, China

[c] School of Food Science and Nutrition, University of Leeds, Leeds, LS2 9JT, UK

[1] The first two authors contributed equally to this paper.

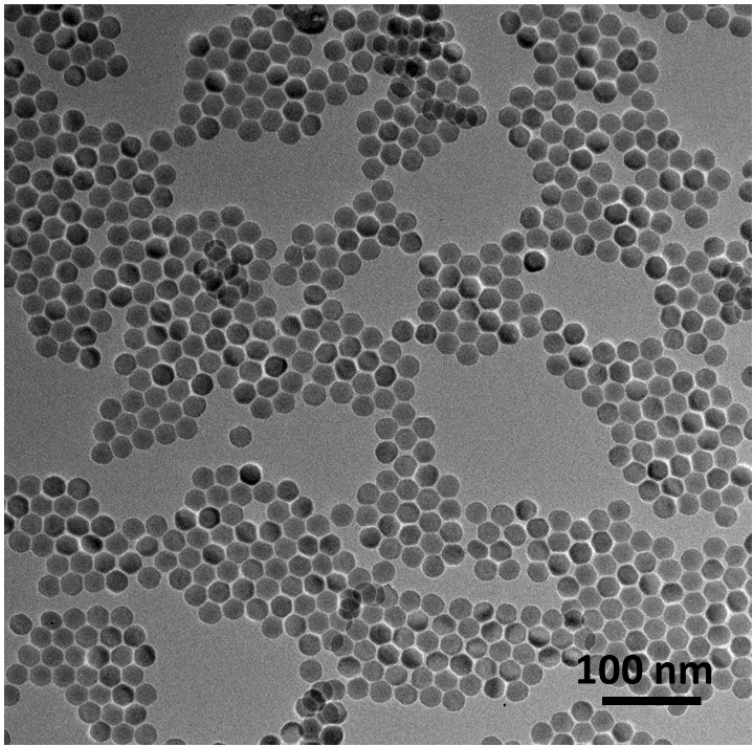

Fig. S1 TEM images of UCNPs dispersed in cyclohexane.

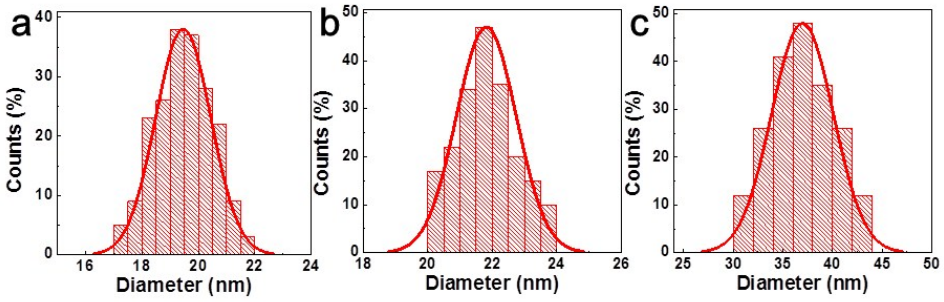

Fig. S2. Geometric mean diameters of UCNPs (a), UCNP@$Al(OH)_3$ nanoparticles (b) and UCNP@$Al(OH)_3$/Au nanohybrids (c). The size analysis of the nanoparticles is through TEM images, and the number of particles counted for size analysis as N=200.

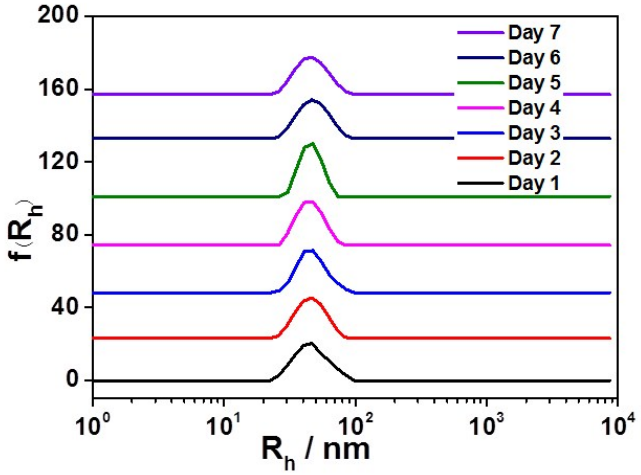

	Day 1	Day 2	Day 3	Day 4	Day 5	Day 6	Day 7
Average size (nm)	47.74	46.88	47.74	46.15	46.30	49.06	47.84

Fig. S3. Dynamic light scattering (DLS) data of UCNP@$Al(OH)_3$/Au nanohybrids after being dispersed in aqueous solution for different times. The slight increase of the diameter compared with the results of TEM can be attributed to the interaction of solvent molecules with the surface of particles.

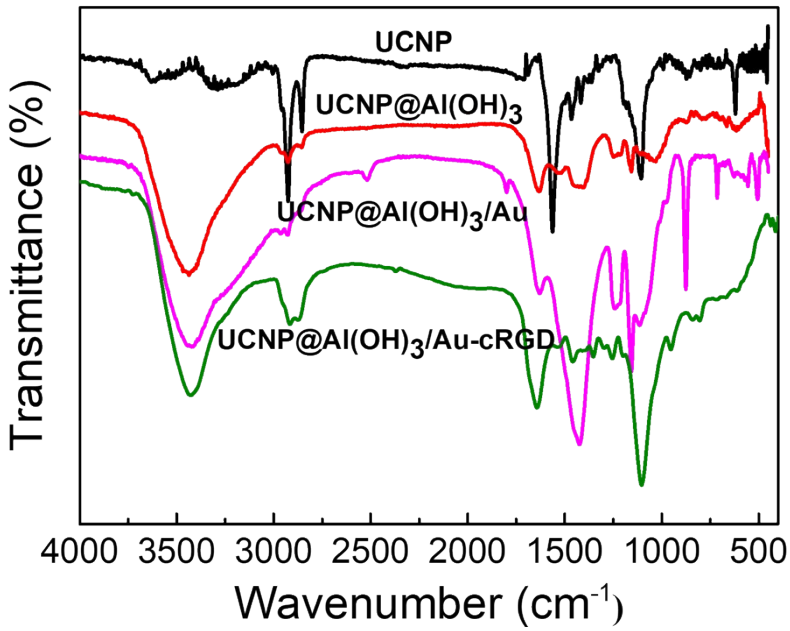

Fig. S4. FTIR spectra of UCNPs, UCNP@$Al(OH)_3$ nanoparticles, UCNP@$Al(OH)_3$/Au nanohybrids and UCNP@$Al(OH)_3$/Au-cRGD nanohybrids.

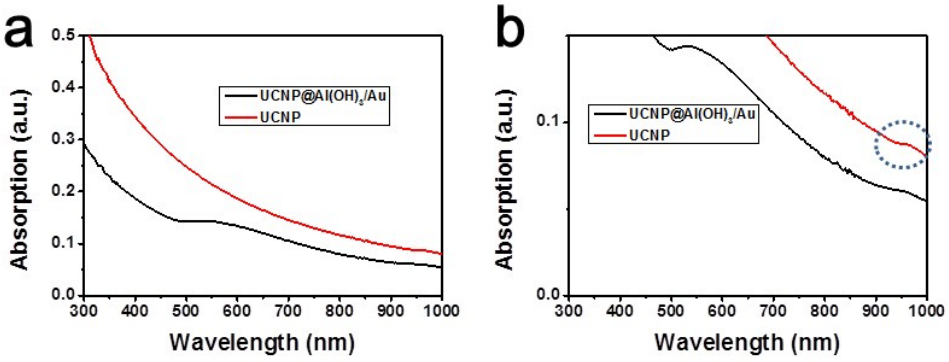

Fig. S5. UV-vis-NIR absorption spectra of UCNPs and UCNP@$Al(OH)_3$/Au nanohybrids.

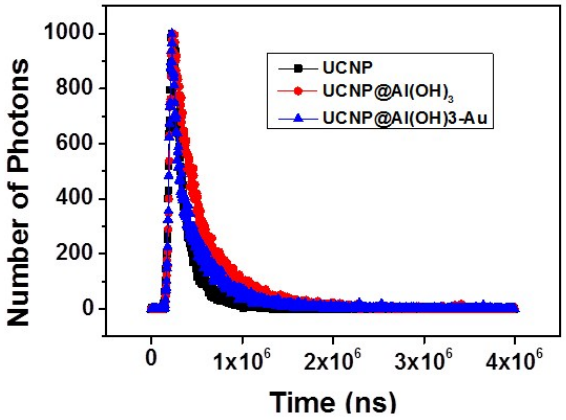

	UCNP	UCNP@Al(OH)$_3$	UCNP@Al(OH)$_3$-Au
B_1	845.188	498.421	515.611
B_2	265.292	529.659	501.821
τ_1	$1.039*10^{-4}$	$1.666*10^{-4}$	$5.499*10^{-5}$
τ_2	$2.637*10^{-4}$	$4.189*10^{-4}$	$3.469*10^{-4}$

Fig. S6. Fluorescence decay trace from UCNP nanoparticles, UCNP@Al(OH)$_3$ nanoparticles and UCNP@Al(OH)$_3$/Au nanohybrids.

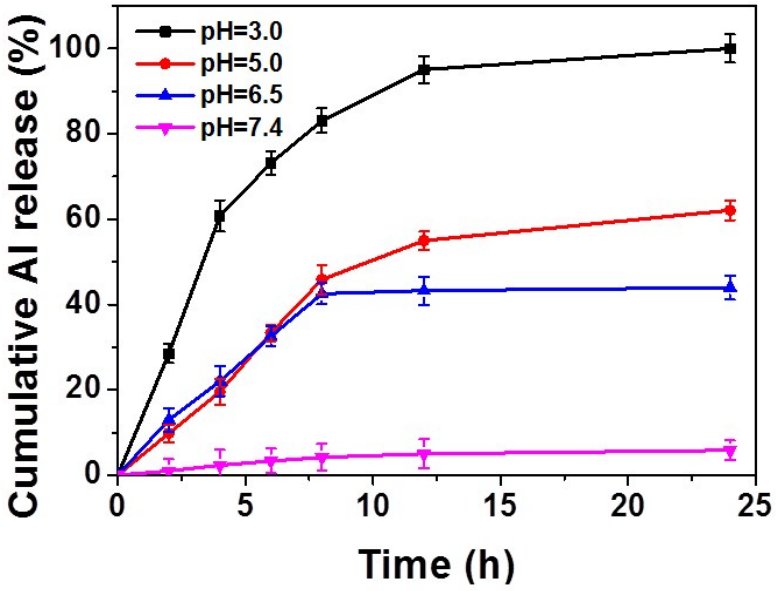

Fig. S7. The release amounts of Al^{3+} from UCNP@Al(OH)$_3$ nanoparticles in PBS with different pH analyzed by ICP.

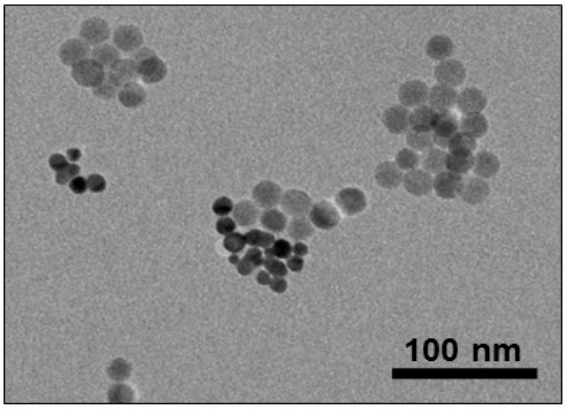

Fig. S8. TEM images of Au NPs separated from UCNP@$Al(OH)_3$/Au nanohybrids dispersed in PBS (pH=5.0).

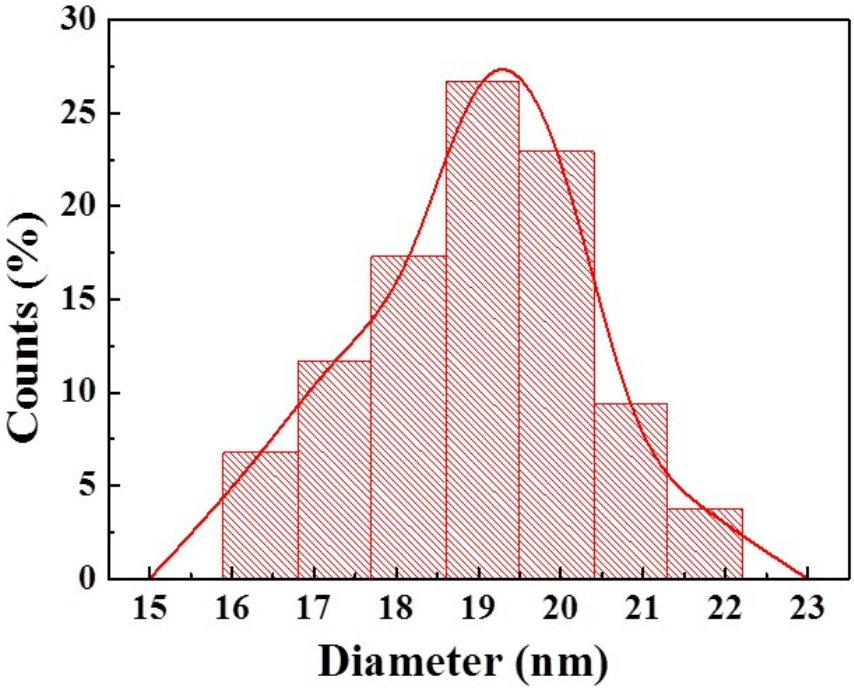

Fig. S9. Geometric mean diameters of UCNP@$Al(OH)_3$/Au nanohybrids after decomposed in acidic environments. The size analysis of the nanoparticles is through TEM images, and the number of particles counted for size analysis as N=200.

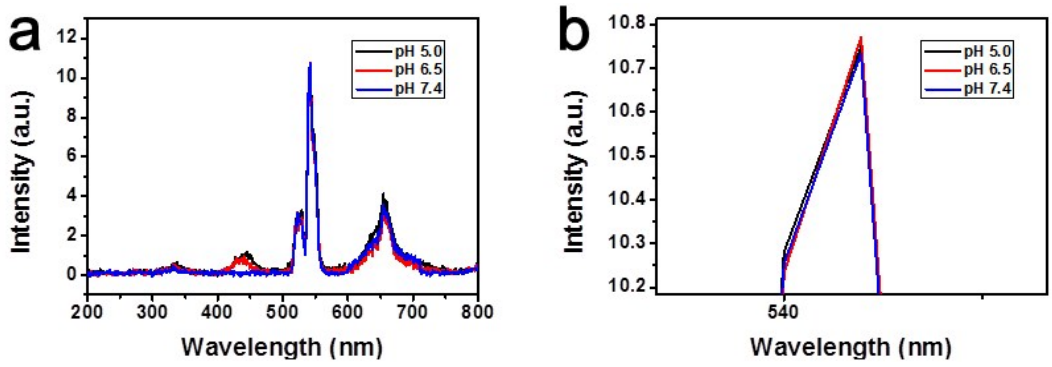

Fig. S10. UCL emission spectra of UCNP nanoparticles dispersed in PBS at various pH (5.0, 6.5 and 7.4) (a) and the corresponding amplifying parts around 540 nm (b).

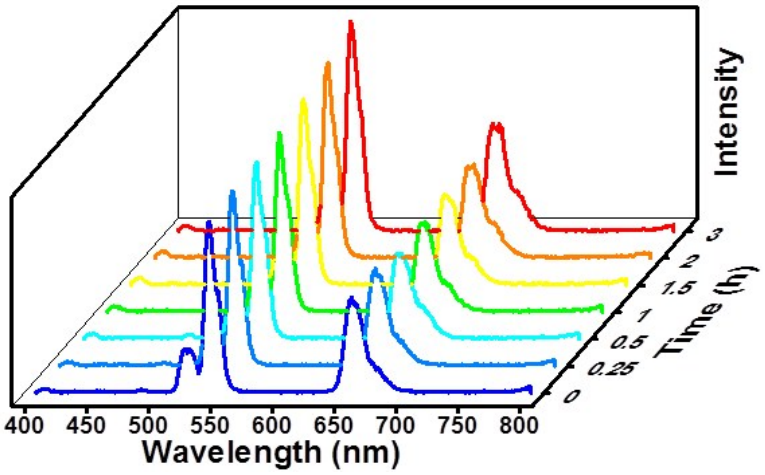

Fig. S11. UCL emission spectra of UCNP@$Al(OH)_3$/Au nanohybrids after being dispersed in acidic solution (pH=5.0) for different times.

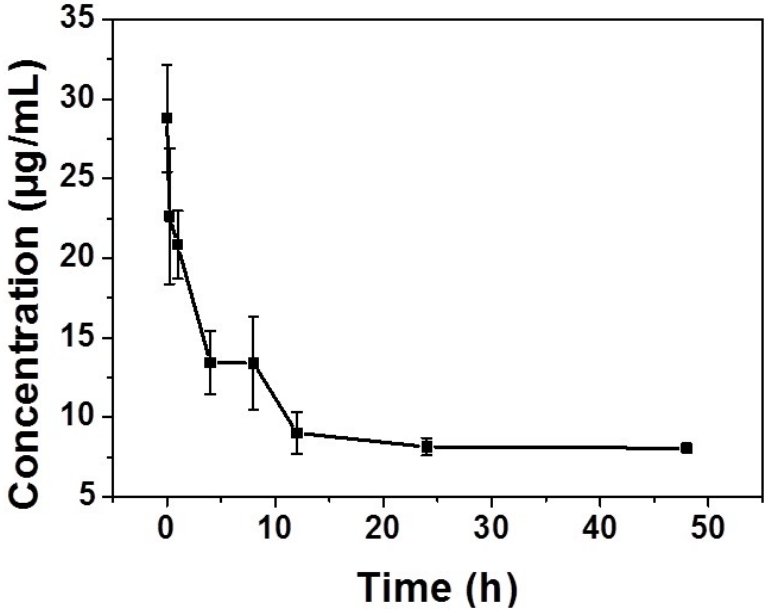

Fig. S12. The blood circulation curve of intravenously injected UCNP@$Al(OH)_3$/Au-cRGD nanohybrids (n = 3). The distribution half-life ($\mathbf{t_{\alpha/2}}$) and elimination half-life ($\mathbf{t_{\beta/2}}$) of UCNP@$Al(OH)_3$/Au-cRGD nanohybrids were 0.55 h and 3.64 h, respectively.

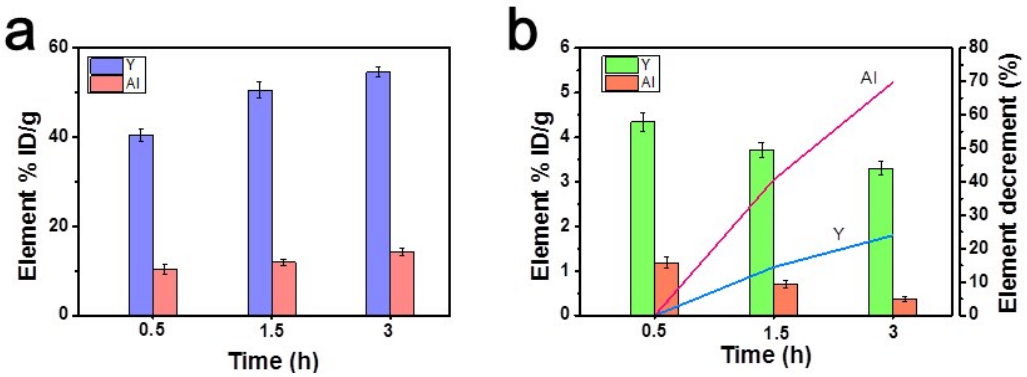

Fig. S13. The biodistribution of Y and Al (% injected dose (ID) of element per gram of tissues) in livers (a) and tumors (b) in 0.5, 1.5, and 3 h of intravenous administrations of UCNP@$Al(OH)_3$/Au-cRGD nanohybrids (n = 3). The curves in (b) demonstrated the decrement of Y and Al in tumors with time passed by.